Electronic Supplementary Information (ESI)

Contiguous Layer Based Metal−Organic Framework with Conjugated π‑Electron Ligand for High Iodine Capture

Tong Xu, Jiantang Li, Mingwei Jia, Guanghua Li and Yunling Liu*

State Key Laboratory of Inorganic Synthesis and Preparative Chemistry, College of Chemistry, Jilin University, Changchun 130012, P. R. China

E-mail: zlr@jlu.edu.cn; yunling@jlu.edu.cn; Fax: +86-431-85168624; Tel: +86-431-85168614

Adsorption and Release of Iodine

The amount of iodine adsorbed on the MOFs at equilibrium was obtained using Eq. (1) The isothermal adsorption curve was linearly fitted to the Langmuir equation Eq. (2) and the Freundlich equation Eq. (3) to obtain the theoretical maximum adsorption capacity of the adsorbent for iodine.

(1) $$Q_e = (C_0 - C_e) \times \frac{V}{w}$$

(2) $$Q_e = \frac{Q_m k_L C_e}{1 + k_L C_e}$$

(3) $$Q_e = k_F C_e^{\frac{1}{n}}$$

In the above equations, Q_e (mg g^{-1}) is the equilibrium adsorption capacity of the adsorbent for iodine when the adsorption reaches equilibrium, and C_0 (mg L^{-1}) is the iodine concentration in the initial solution. C_e (mg L^{-1}) is the iodine concentration in the solution when the adsorption reaches equilibrium. V (mL) is the volume of iodine solution. w (mg) is the mass of the added adsorbent. Q_m (mg g^{-1}) is the theoretical maximum adsorption capacity of the adsorbent for iodine. k_L (L mg^{-1}) is the Langmuir model constant, while k_F (mg g^{-1}) is the Freundlich model constant. n is a linear constant.

Supporting Tables

Table S1. Crystal data and structure refinements for compound **1**.

Compound	Compound **1**
Formula	$C_{30}\ H_{44}\ Cu_3\ N_{16}\ O_{13}$
Mw	1027.43
Temp (K)	173(2)
Wavelength (Å)	0.71073
Crystal system	Monoclinic
Space group	*C*2/*m*
a (Å)	19.7115(10)
b (Å)	26.1902(12)
c (Å)	20.0351(11)
α (°)	90
β (°)	113.054(2)
γ (°)	90
V (Å^3)	9517.0(8)
Z, D_C (Mg/m^3)	8, 1.434
F(000)	4216
θ range (deg)	2.192 - 30.555
reflns collected/unique	60767 / 14851
R_{int}	0.0304
data/restraints/params	14851 / 2 / 398
GOF on F^2	1.119
R^1, wR^2 (I>2σ(I))	0.0474, 0.1736
R^1, wR^2 (all data)	0.0536, 0.1778

Table S2. Selected bond lengths [Å] and angles [°] for compound **1**.

Compound 1			
Cu(1)-O(1)	1.9081(18)	N(6)-Cu(3)-O(4)#2	92.68(8)
Cu(1)-O(2)	1.9148(18)	N(6)-Cu(3)-N(9)#3	177.32(10)
Cu(1)-O(3)	2.276(3)	N(6)-Cu(3)-N(11)	92.51(10)
Cu(1)-N(5)	2.013(2)	O(4)#2-Cu(3)-N(9)#3	88.26(9
Cu(1)-N(2)	2.019(2)	N(9)#3-Cu(3)-N(11)	90.06(10)
Cu(2)-O(1)	1.8981(19)	Cu(2)-O(1)-Cu(1)	122.72(10
Cu(2)-N(3)	1.992(2)	Cu(1)-O(2)-Cu(3)	123.20(10)
Cu(2)-N(8)	2.007(2)	C(21)-O(3)-Cu(1)	128.3(2)
Cu(2)-N(12)#1	2.005(2)	C(21)-O(4)-Cu(3)#2	108.52(18)
Cu(3)-O(2)	1.9143(18)	N(3)-N(2)-Cu(1)	119.44(16)
Cu(3)-O(4)#2	1.9950(19	C(4)-N(2)-Cu(1)	132.96(19)
Cu(3)-N(6)	1.990(2)	N(2)-N(3)-Cu(2)	119.14(16)
Cu(3)-N(9)#3	1.994(2)	C(5)-N(3)-Cu(2)	132.66(18)
Cu(3)-N(11)	2.235(3)	N(6)-N(5)-Cu(1)	119.66(16)
O(1)-Cu(1)-O(2)	175.01(10)	C(9)-N(5)-Cu(1)	132.42(18)
O(1)-Cu(1)-O(3)	96.29(10)	N(5)-N(6)-Cu(3)	120.32(16)
O(1)-Cu(1)-N(2)	86.29(8)	C(10)-N(6)-Cu(3)	131.27(18)
O(1)-Cu(1)-N(5)	92.26(9)	N(9)-N(8)-Cu(2)	123.78(16)
O(2)-Cu(1)-O(3)	88.68(10)	C(14)-N(8)-Cu(2)	128.27(18)
O(2)-Cu(1)-N(2)	92.63(8)	N(8)-N(9)-Cu(3)#1	120.28(16)
O(2)-Cu(1)-N(5)	87.75(8)	C(15)-N(9)-Cu(3)#1	131.79(19)
N(2)-Cu(1)-O(3)	99.11(12)	N(12)-N(11)-Cu(3)	121.73(18)
N(5)-Cu(1)-O(3)	93.28(12)	C(19)-N(11)-Cu(3)	130.6(2)
N(5)-Cu(1)-N(2)	167.61(11)	N(11)-N(12)-Cu(2)#3	118.61(18)
O(1)-Cu(2)-N(3)	87.69(9)	C(20)-N(12)-Cu(2)#3	132.8(2)
O(1)-Cu(2)-N(8)	89.93(8)	O(4)#2-Cu(3)-N(11)	86.15(9)
O(1)-Cu(2)-N(12)#1	171.89(10)	O(2)-Cu(3)-N(11)	98.76(9)
N(3)-Cu(2)-N(8)	168.14(10)	O(2)-Cu(3)-N(9)#3	90.67(8)
N(3)-Cu(2)-N(12)#1	92.98(9)	O(2)-Cu(3)-N(6)	88.18(8)
N(8)-Cu(2)-N(12)#1	91.01(9)	O(2)-Cu(3)-O(4)#2	174.97(9)

Symmetry transformations used to generate equivalent atoms:
#1 x-1/2,-y+1/2,z #2 -x-1/2,-y+1/2,-z #3 x+1/2,-y+1/2,z #4 x,-y+1,z #5 x,-y,z
#6 -x,y,-z+1 #7 -x+1,y,-z

Table S3. Comparison of iodine solution adsorption in different materials.

Name	I_2 uptake (g/g)	Ref.
HCOF-1	2.1	1
MFM-300(Sc)	1.54	2
HMTI-1	1.5	3
BC@Dopa-ZIF	1.31	4
MFM-300(Fe)	1.29	2
UiO-66-PYDC	1.25	5
$\{[Zn_3(dl\text{-}lac)_2(pybz)_2]\cdot 2.5DMF\}_n$	1.01	6
MFM-300(Al)	0.94	2
COF-5d	0.91	7
NOP-54	0.89	8
NOP-55	0.81	8
Fe_3O_4/COF-5d	0.797	9
$[(Cu_4I_4)CuL_2(Dabco)_{1.5}]\cdot 10H_2O\cdot 2DMF$	0.77	10
FCMP-600@2	0.729	11
FCMP-600@1	0.55	11
FCMP-600@4	0.539	11
FCMP-600@3	0.52	11
NTP	0.429	12
$Cd_3(TBP)_4$	0.438	13
MIL-101-NH_2	0.311	14
JLU-Liu32	0.29	15
$\{[Mn_2(oxdz)_2(tpbn)(H_2O)_2]\cdot 2C_2H_5OH\}_n$	0.168	16
Micro-Cu_4I_4-MOF	0.13	17
Compound 1	1.15	***This work***

Table S4. The Langmuir and Freundlich parameters for iodine adsorption on compound **1**.

Langmuir			Freundlich		
Q_m (mg g^{-1})	k_L (L mg^{-1})	R^2	k_F (mg g^{-1})	n	R^2
1050.18	**0.017**	**0.85**	**219.41**	**4.54**	**0.98**

Supporting Figures

Fig. S1 The ligand p-tr$_2$ph(1,4-phenylene-4,4'-bis(1,2,4-triazole)).

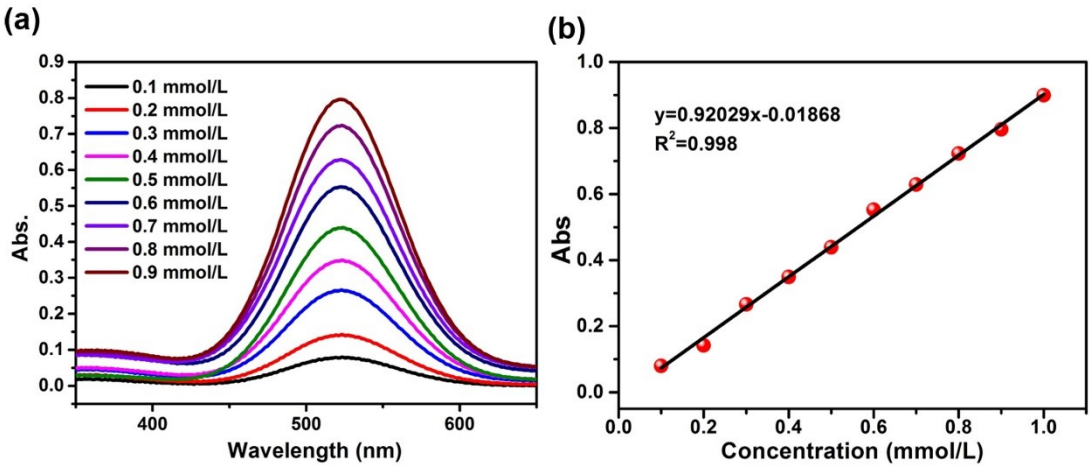

Fig. S2 (a) UV-Vis spectra of iodine in cyclohexane; (b) The standard curve of iodine in cyclohexane.

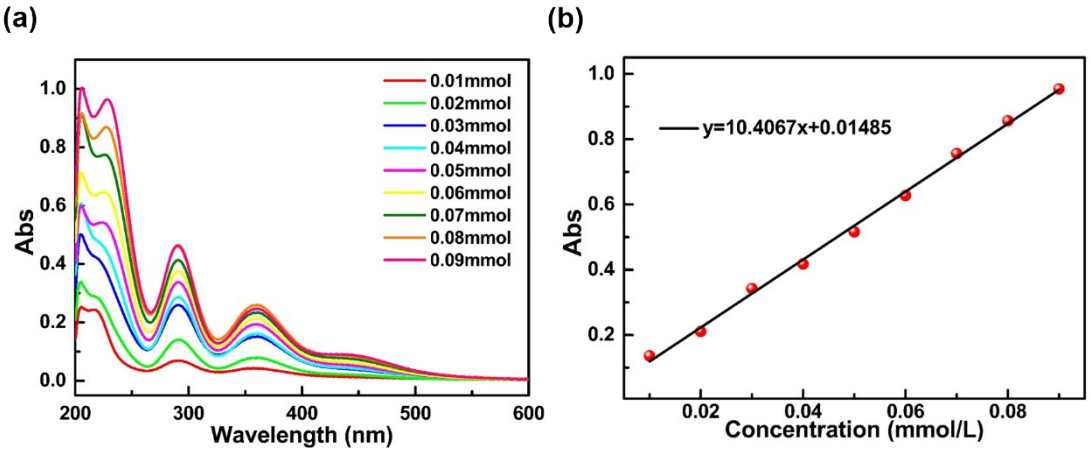

Fig. S3 (a) UV-Vis spectra of iodine in ethanol; (b) The standard curve of iodine in ethanol.

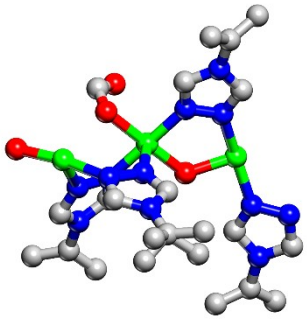

Fig. S4 The asymmetric structural motif of compound **1**.

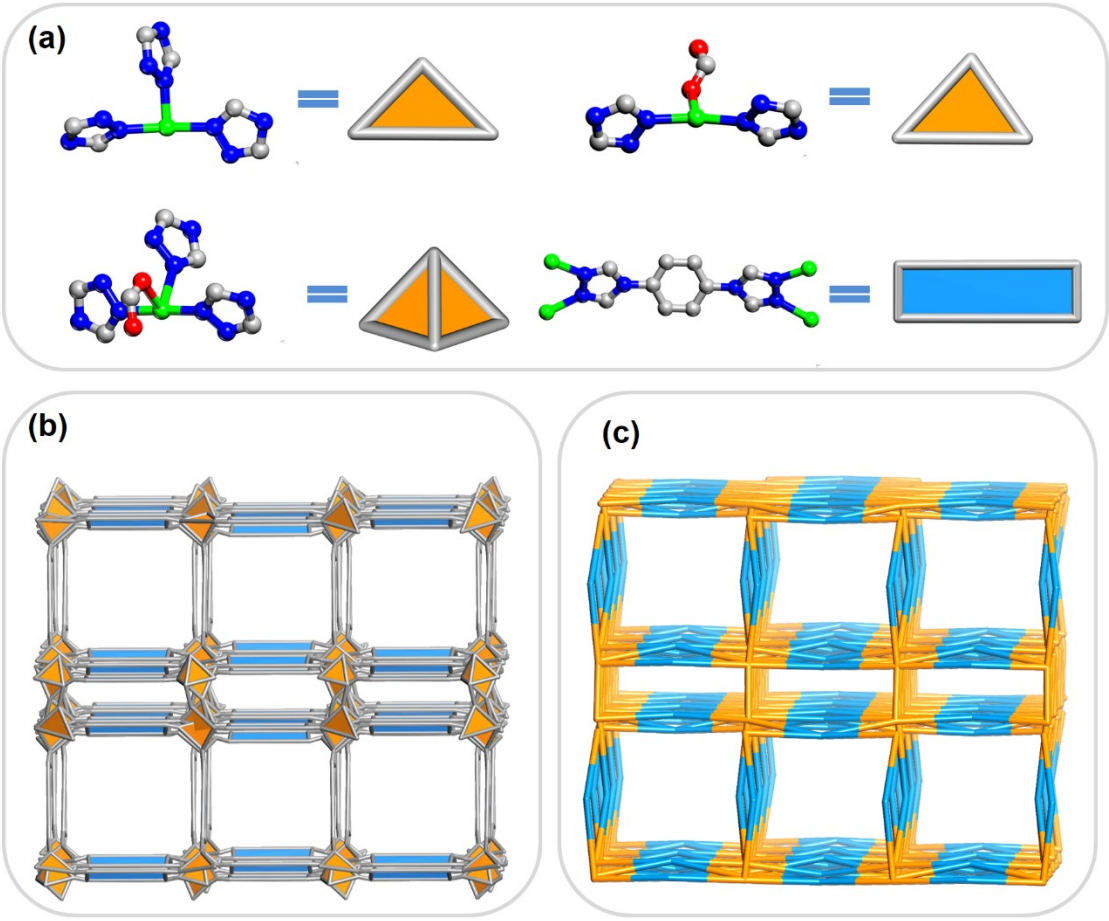

Fig. S5 Single-crystal structure of compound **1**: (a) quaternary SBUs consisting of ligand and metal cores, (b) Polyhedral view of the framework, (c) The new type of topology.

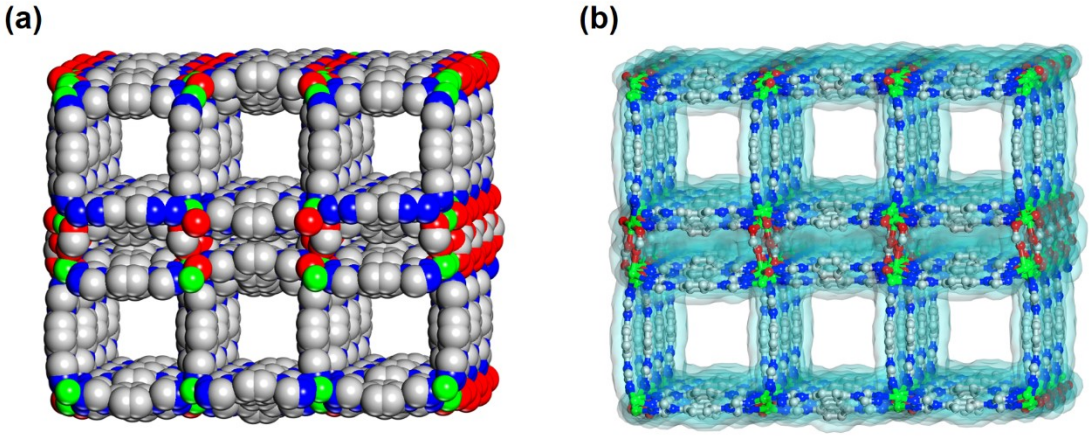

Fig. S6 (a) Space-filling models of compound **1** along [100] direction, (b) The illustration of multiple pores for compound **1** displayed by connolly surface areas.

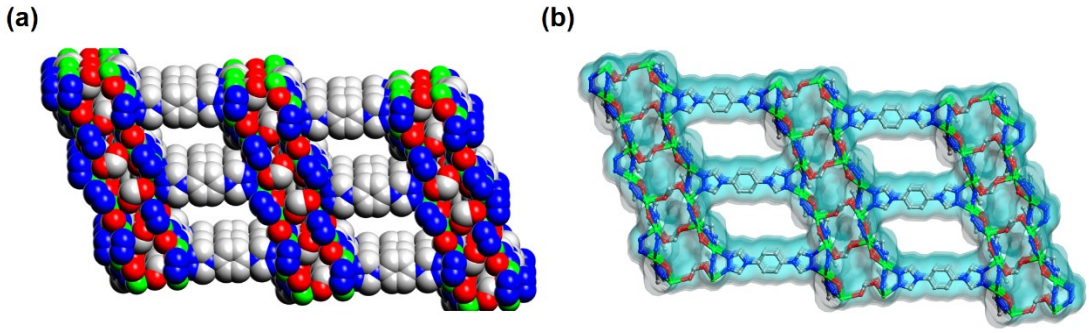

Fig. S7 (a) Space-filling models of compound **1** along [010] direction, (b) The illustration of multiple pores for compound **1** displayed by connolly surface areas.

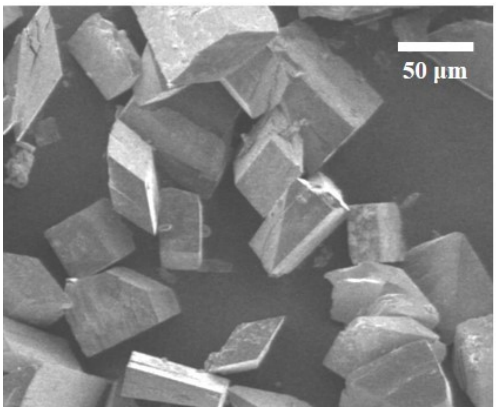

Fig. S8 The SEM image of the compound **1**.

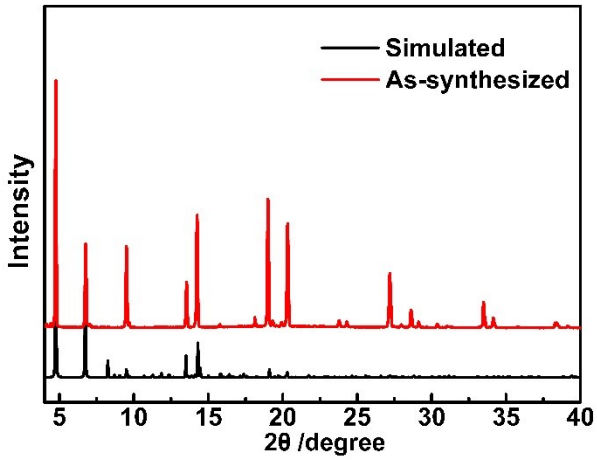

Fig. S9 PXRD patterns of compound **1** for the simulated and as-synthesized.

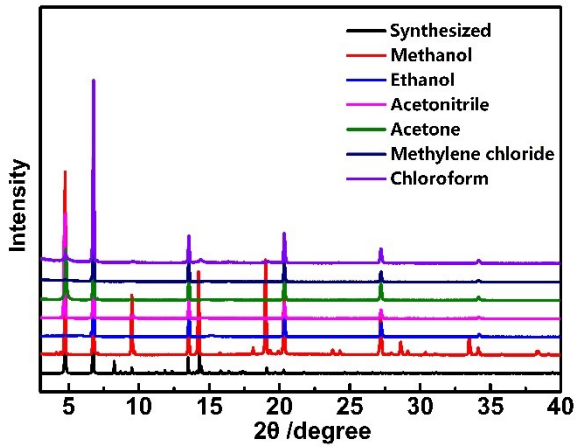

Fig. S10 PXRD patterns of compound **1** for different solvent-exchanged samples.

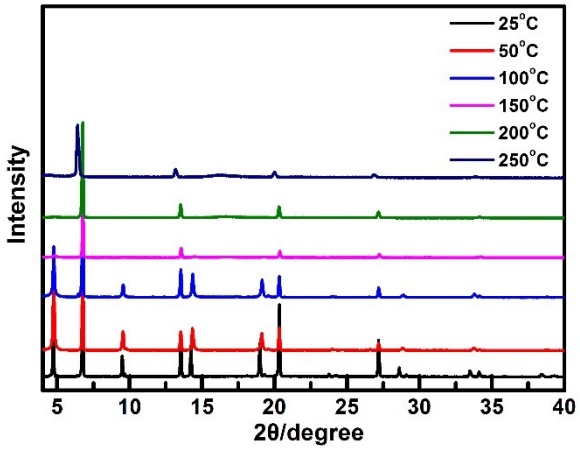

Fig. S11 Variable-temperature PXRD patterns of compound **1**.

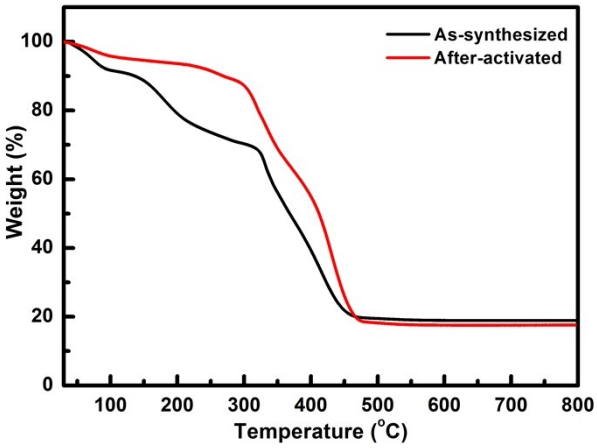

Fig. S12 Thermogravimetric analysis curves of compound **1** for the as-synthesized and after-activated samples.

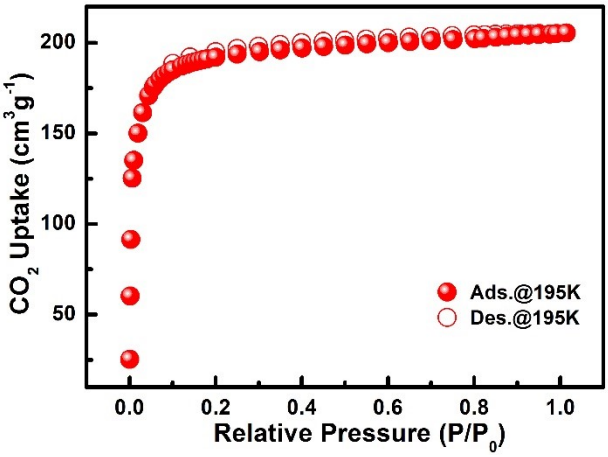

Fig. S13 195 K CO_2 sorption isotherms for compound **1**.

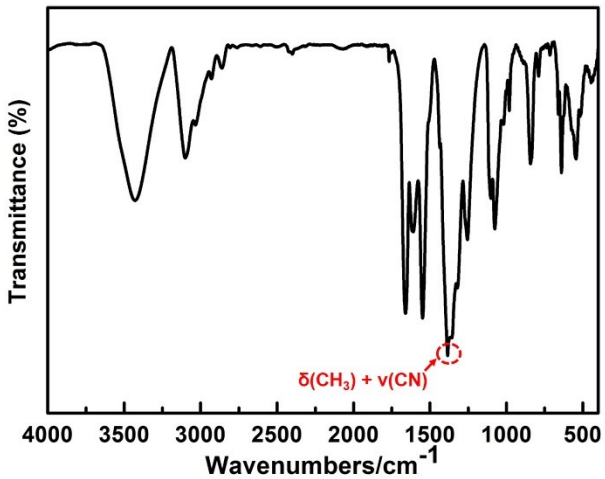

Fig. S14 FTIR spectrum of compound **1**.

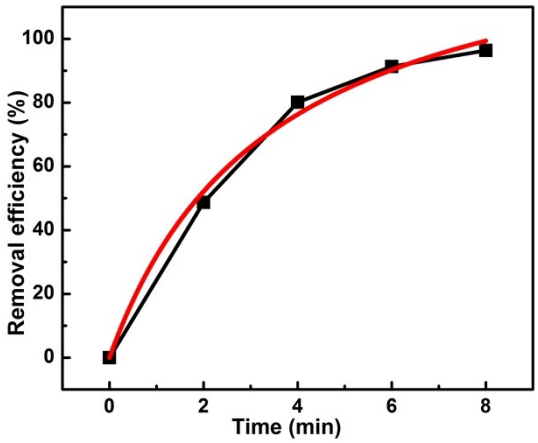

Fig. S15 Plots of pseudo-second-order kinetics.

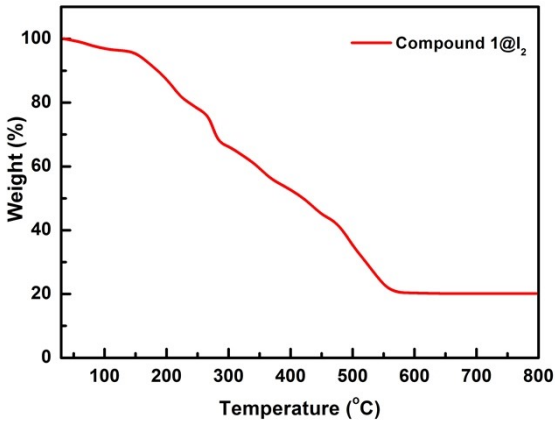

Fig. S16 Thermogravimetric analysis curves of I_2-adsorbed samples.

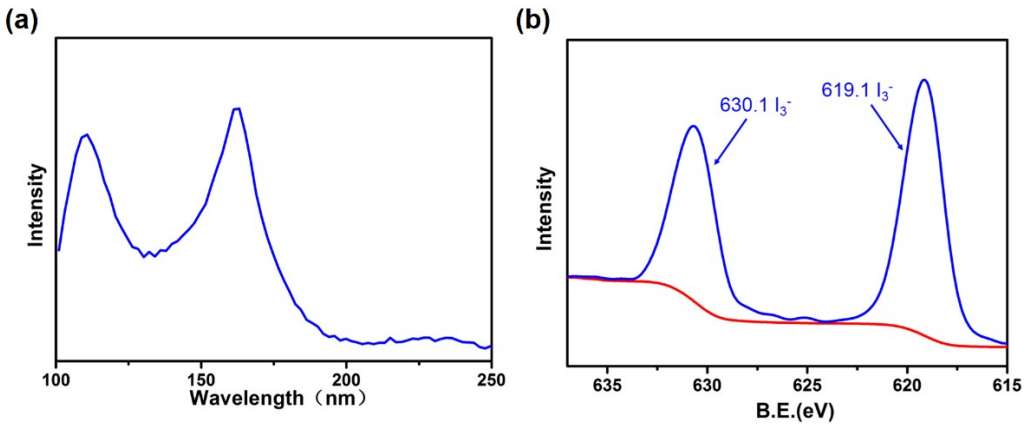

Fig. S17 (a) Raman and (b) XPS spectra of compound **1** after I_2 adsorption.

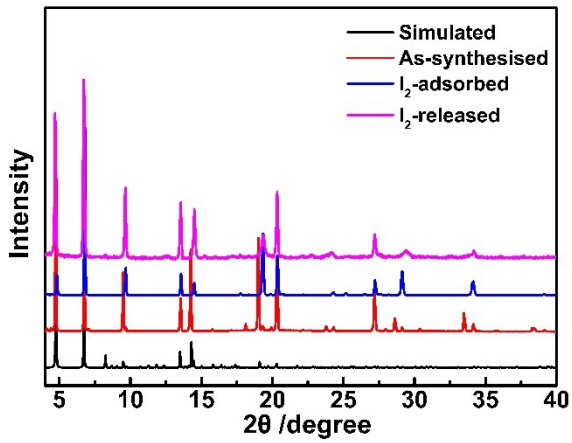

Fig. S18 PXRD patterns of compound **1** for simulated, as-synthesized, I2-adsorbed and after cycles samples.

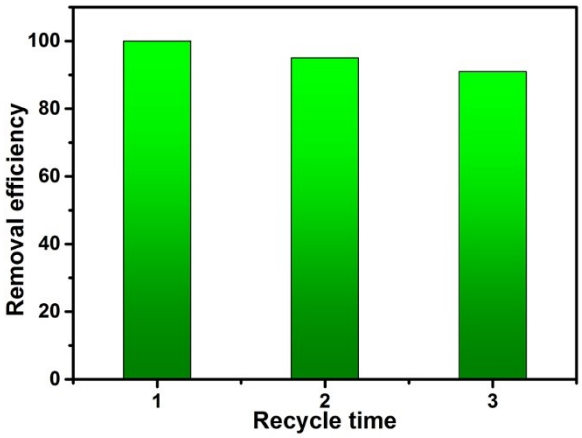

Fig. S19 Number of iodine adsorption cycles on removal efficiency of compound **1**.

Reference

1. L. Hashemi and A. Morsali, *CrystEngComm*, 2012, **14**, 779-781.
2. A. N. Au-Duong and C. K. Lee, *Cryst. Growth Des.*, 2018, **18**, 356-363.
3. Z. Wang, Y. Huang, J. Yang, Y. Li, Q. Zhuang and J. Gu, *Dalton Trans.*, 2017, **46**, 7412-7420.
4. M. H. Zeng, Q. X. Wang, Y. X. Tan, S. Hu, H. X. Zhao, L. S. Long and M. Kurmoo, *J. Am. Chem. Soc.*, 2010, **132**, 2561-2563.
5. S. Q. Xu, T. G. Zhan, Q. Wen, Z. F. Pang and X. Zhao, *ACS Macro Lett.*, 2016, **5**, 99-102.
6. D. Chen, Y. Fu, W. Yu, G. Yu and C. Pan, *Chem. Eng.J.*, 2018, **334**, 900-906.
7. Y. Liao, J. Li and A. Thomas, *ACS Macro Lett.*, 2017, **6**, 1444-1450.
8. M. Jia, J. Li, S. Che, L. Kan, G. Li and Y. Liu, *Inorg. Chem. Front.*, 2019, **6**, 1261-1266.
9. G. Li, C. Yao, J. Wang and Y. Xu, *Scientific Reports*, 2017, **7**, 13972.
10. H. Ma, J. J. Chen, L. Tan, J. H. Bu, Y. Zhu, B. Tan and C. Zhang, *ACS Macro Lett.*, 2016, **5**, 1039-1043.
11. P. Cui, L. Ren, Z. Chen, H. Hu, B. Zhao, W. Shi and P. Cheng, *Inorg. Chem.*, 2012, **51**, 2303-2310.

12. C. Falaise, C. Volkringer, J. Facqueur, T. Bousquet, L. Gasnot and T. Loiseau, *Chem. Commun.*, 2013, **49**, 10320-10322.
13. S. Yao, X. Sun, B. Liu, R. Krishna, G. Li, Q. S. Huo and Y. L. Liu, *J. Mater. Chem. A*, 2016, **4**, 15081-15087.
14. N. X. Zhu, C. W. Zhao, J. C. Wang, Y. A. Li and Y. B. Dong, *Chem. Commun.*, 2016, **52**, 12702-12705.
15. Y. Lin, X. Jiang, S. T. Kim, S. B. Alahakoon, X. Hou, Z. Zhang, C. M. Thompson, R. A. Smaldone and C. Ke, *J. Am. Chem. Soc.*, 2017, **139**, 7172-7175.
16. A. Gogia, P. Das, and S. K. Mandal, *ACS Appl. Mater. Interfaces*, 2020, **12**, 46107−46118.
17. X. Zhang, I. da Silva, H. G. W. Godfrey, S. K. Callear, S. A. Sapchenko, Y. Cheng, I. Vitórica-Yrezábal, M. D. Frogley, G. Cinque, C. C. Tang, C. Giacobbe, C. Dejoie, S. Rudić, A. J. Ramirez-Cuesta, M. A. Denecke, S. Yang and M. Schröder, *J. Am. Chem. Soc.*, 2017, **139**, 16289-16296.